Journal of Materials Chemistry C

COMMUNICATION

View Article Online
View Journal | View Issue

Silver nanowire transparent conducting paper-based electrode with high optical haze†

Cite this: J. Mater. Chem. C, 2014, 2, 1248

Received 3rd September 2013
Accepted 5th October 2013

DOI: 10.1039/c3tc31726a

www.rsc.org/MaterialsC

Colin Preston,‡[a] Zhiqiang Fang,‡[a] Joseph Murray,[bc] Hongli Zhu,[a] Jiaqi Dai,[a] Jeremy N. Munday*[bc] and Liangbing Hu*[a]

In this study we report a novel, rationally designed, solution based silver nanowire (Ag NW) paper hybrid that demonstrates a flexible, low cost, and scalable device ready transparent conducting electrode (TCE) with exceptional and stable optoelectronic properties. Its high transmittance (91%) and low sheet resistance (13 Ω sq^{-1}) represent the highest reported figure of merit value for solution based TCEs according to conventional models. We also thoroughly investigate the diffuse light scattering properties of our Ag NW paper with various techniques that elucidate the total optical haze as well as the diffuse scattering angle distribution for this TCE. Through a simulation of the impact the optical properties of TCEs have on the light absorption in the conversion layers for various thin film solar cells, we demonstrate that our Ag NW paper induces greater light absorption than ITO for each simulated thin film solar cell.

Introduction

Transparent conducting electrodes (TCEs) are critical to the manufacture and performance of thin film photovoltaic devices. Optimal TCEs must possess a high transparency to maximize the absorbed light in a solar cell's conversion layer and possess a high conductivity to minimize ohmic loss.[1,2] The current thin film photovoltaic market is dominated by conducting metal oxides such as indium tin oxide (ITO) for the TCE material due its high conductivity (10 Ω sq^{-1}) and high transparency (85%).[3,4] Despite the good transparency and conductivity of ITO films, the high cost of indium, the inherent brittleness of its ceramic structure, and its costly deposition technique prevents ITO from being amenable to low cost manufacturing or flexible solar modules.[5,6] Recent studies have investigated alternatives to ITO such as carbon nanotubes (CNT),[7–10] graphene,[11–13] and metallic nanostructures.[14–17] These novel materials form a TCE through a solution based process, which enables the highly economical manufacturing method of roll-to-roll printing for flexible electronics.[18] Ink-based films comprised of conductive percolation networks of Ag NWs with high aspect ratios are particularly promising, because they report exceptional transparency and conductivity that can compete with and even surpass the electrical and optical properties of ITO TCEs.[14–16,18–20] The most common substrate to host flexible electronics is plastic; however recent studies report paper substrates with high transparency that are amenable to hosting printed electronics.[24,25] Printing flexible electronics on paper rather than plastic substrates further bolsters economical production due to the renewable, environmentally friendly, light-weight, mechanically flexible, and disposable properties of paper.[21–23] A common problem that hinders the performance of printed TCEs is delamination of the conductive film from the substrate after repeated rubbing or induced strain. Studies show that embedding a conductive Ag NW network onto the surface of a flexible substrate stabilizes it and keeps it from delaminating, but plastics require a pre-treatment of its surface before the Ag NW layer can be embedded.[36,37]

In this study we introduce a novel TCE structure that consists of an Ag NW network embedded onto the surface of a transparent paper substrate through a simple, novel lamination process without the need for any pre-treatments. By embedding the Ag NW network onto the surface of the transparent paper substrate through a wet-lamination process, the TCE possesses a high mechanical stability while retaining its conductivity. Fig. 1 schematically illustrates the design for this new structure. This Ag NW paper electrode is low cost, renewable, durable, and demonstrates high optoelectronic performance. In addition to these compelling attributes, Ag NW transparent paper exhibits high optical haze, which makes it a most suitable alternative to ITO TCEs in flexible thin film photovoltaic modules. Optical haze is the degree of diffuse light scattering through the TCE

[a]Department of Materials Science and Engineering, University of Maryland College Park, College Park, Maryland, 20742, USA. E-mail: binghu@umd.edu
[b]Department of Electrical and Computer Engineering, University of Maryland, College Park, Maryland, 20742, USA. E-mail: jnmunday@umd.edu
[c]The Institute for Research in Electronics and Applied Physics, University of Maryland, College Park, Maryland, 20742, USA

† Electronic supplementary information (ESI) available. See DOI: 10.1039/c3tc31726a

‡ These authors contributed equally to the work featured in the manuscript.

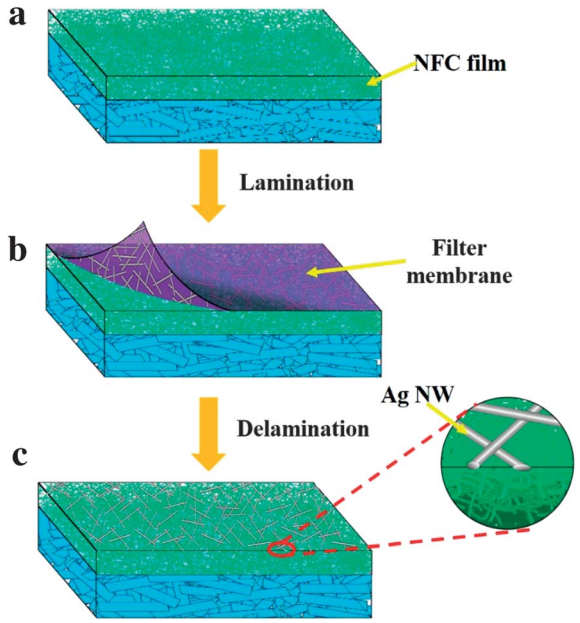

Fig. 1 Schematic of Ag NW network embedded in a nanopaper surface on the transparent paper. (a) Nanofibrillated cellulose was filtered through TEMPO-treated paper to form a smooth surface, (b) with a novel lamination process, a filtered Ag NW network is embedded in the smooth NFC surface, and (c) the final structure is a uniform Ag NW network embedded onto the surface of transparent paper.

films. Light scattering enhances the path length of light transmitted through the solar conversion layer of thin film photovoltaic devices, which enhances the light absorption by the conversion layer and thus the solar efficiency of the photovoltaic device. Ag NW films are reported to exhibit significant diffuse light scattering properties that depend on the density of the wires in the network and their diameter.[26] Transparent paper is also reported to exhibit significantly high optical haze that depend on the nanofibril cellulose network within the network.[24] Investigations into the total diffuse scattering is previously reported for Ag NW films and paper individually, but there are no reports of the angular distribution of light scattered through these respective layers, nor are there any reports of the optical properties for a composite TCE of a Ag NW embedded on a transparent paper substrate. Along with introducing a novel TCE structure with nominal optoelectronic properties, this study also investigates the unique optical haze properties of the Ag NW transparent paper, and directly correlates these optical properties to better light absorption in thin film solar conversion layers as compared to similar devices consisting of ITO.[27]

Results and discussion

Synthesis of Ag NW transparent conducting paper electrode

Bleached sulfate softwood pulp extracted from southern yellow pine was dispersed in distilled water containing sodium bromide and TEMPO, and then disintegrated in the solution with a Turrax mixer. A portion of the TEMPO-treated pulp was passed through a Microfluidizer to produce nanofibrillated cellulose (NFC). The NFC was then filtered into a thin wet NFC film for the purpose of getting high smoothness for the transparent paper. TEMPO-treated pulp was then filtered through the NFC film to form a wet transparent paper substrate. The transparency of this substrate reaches 96% at a wavelength of 550 nm, as illustrated in the ESI (S1).† A Ag NW suspension was then filtered into a homogenous transparent film, and then laminated with a pure NFC layer to the transparent paper. Fig. 2 depicts the Ag NW transparent paper electrode sample, with Fig. 2(a) demonstrating a visibly homogenous Ag NW network on the transparent paper with good transparency. It is also clear that the light scattering through this electrode is very high; the transparency through the electrode diminishes rapidly and images farther from the surface appear very cloudy. Fig. 2(b) is an SEM image demonstrating that the Ag NW consists of long wires with a diameter of 100 nm. As previously reported, this larger diameter for the Ag NWs enables greater light scattering.[26] The long Ag NW length enables a large percolation network while still enabling a high transparency for the Ag NW network, and is depicted in the SEM image of the electrode surface in Fig. 2(d).[4,15,28] It is important to note the obvious embedding of the Ag NWs into the transparent paper surface, which stabilizes the mechanical properties of the conducting layer and prevent delamination. Fig. 2(c) further demonstrates this embedded nature of the Ag NW into the surface of the transparent paper, with a clear depiction of the larger transparent paper substrate thickness compared to the Ag NW network.

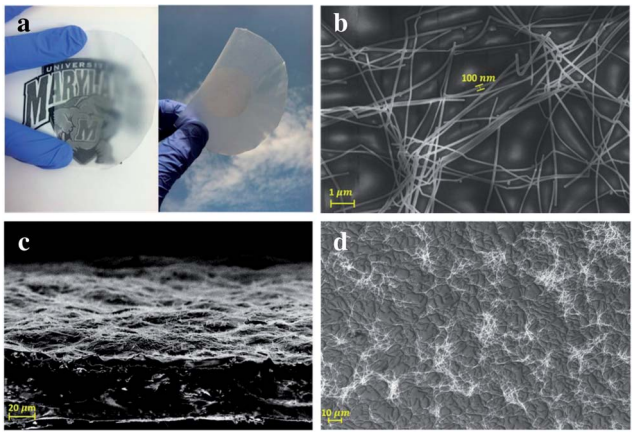

Fig. 2 (a) Optical image of Ag NW transparent paper; (b) SEM of Ag NW with diameter of 100 nm; (c) SEM of cross-section of Ag NW transparent paper; (d) top view of Ag NW transparent paper demonstrating embedded Ag NW network.

Properties of Ag NW paper

Optoelectronic performance. To verify the initial observations of the high transparency of the Ag NW transparent paper electrode, a UV-Vis spectrometer with an integrating sphere was used to measure the total transmittance of the entire TCE. The total electrode transmittance with respect to the wavelength is depicted in Fig. 3(a). At a wavelength of 550 nm the total

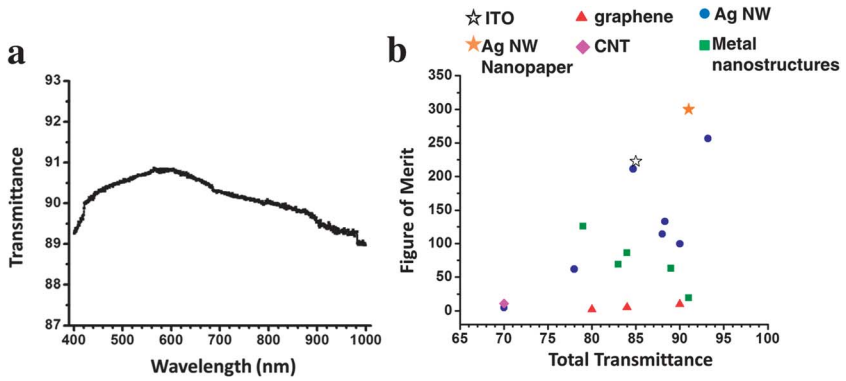

Fig. 3 (a) Total transmittance *versus* wavelength of Ag NW paper; (b) figure of merit *versus* total transmittance for previous TCE reports, ITO, and our Ag NW paper.[15,17,29–35]

transmittance of the TCE is about 91%. This transparency is among the highest reported for TCEs. This value depends on both the optical properties of the substrate as well as the Ag NW network; the nanowires have minimal impact on the transmittance of the composite structure, yet change the paper from insulating to highly conductive. The sheet resistance of this Ag NW transparent conducting paper electrode was measured as 13 $\Omega\ \mathrm{sq_{cm}}^{-1}$.

To evaluate the performance for this TCE, the contemporary figure of merit for transparent electrodes composed of nanostructured films with a thickness below the percolation limit was used to relate the total transmittance at 550 nm and the sheet resistance in eqn (1):[28]

$$\%T = \left(1 + \frac{188.5}{R_S}\frac{\sigma_{optical}}{\sigma_{DC}}\right)^{-1} \rightarrow \frac{\sigma_{DC}}{\sigma_{optical}} = \text{f.o.m.} \quad (1)$$

where σ_{DC} represents the DC conductivity of the bulk material, $\sigma_{optical}$ representing the optical conductivity, $\%T$ representing the transparency at 550 nm, and R_S representing the sheet resistance. Fig. 3(b) displays a comparative review of previously reported figures of merit for various TCEs of various compositions including CNTs;[30] graphene;[31] and ink based metallic networks composed of copper nanowires,[32] gold nanowires,[32] and silver nanowires.[15,17,29,32–34] According to this comparison, our Ag NW transparent conducting paper electrode has a much greater figure of merit than ITO and has the highest figure of merit for solution based TCEs. It is important to note that the previously reported Ag NW TCEs from ink based solutions normalize their optical properties to eliminate the impact of the substrate the networks are deposited on. The figure of merit for our Ag NW transparent conducting electrode includes the substrate within the evaluation of the TCE performance; therefore, it as an accurate performance metric within a device rather than as an isolated Ag NW film. Despite the possible reduction in optoelectronic performance that may occur when evaluating the Ag NW in conjunction with the substrate, our Ag NW transparent conducting paper still possesses the highest reported figure of merit TCEs fabricated with a conventional solution based process. This result is due to the uniform Ag NW network enabled by a filtration onto the transparent paper substrate and the subsequent mechanically pressed NW junctions during the lamination process. In addition the performance was maintained even after several pealing tests with scotch tape (S2).† This demonstrates the high resistance to delamination of the Ag NW transparent paper due to the embedded nanostructures.

Haze properties. The total diffuse scattering, or diffuse optical haze, of an ITO sample sputtered on soda-lime glass, a transparent paper substrate, and the Ag NW paper was measured with a UV-Vis spectrometer with an integrating sphere. The mechanism for haze measurements with an integrating sphere is depicted in the ESI (S3).† The optical haze for the ITO film on soda lime glass is very small (1% at 550 nm), as depicted in Fig. 4(d). The optical haze for the transparent paper reaches 59% at 550 nm (Fig. 4(e)), and the optical haze for the Ag NW transparent paper slightly surpasses 65% at 550 nm (Fig. 4(f)). These values are accurate determinations of the total optical haze through each sample but do not detail the exact behavior of the diffuse scattered light.

An additional experiment to determine the angular distribution of the diffusely scattered light through a surface was conducted to expound upon the optical haze values measured by the UV-Vis spectrometer. The angular distribution of the transmitted light emitted from a source normal to the surface is separated into an non-deflected component and a diffuse component that extends over all transmitted scattering angles.[38] For surfaces like ITO on optically smooth glass, the specular coherent component dominates the angular distribution and displays an extremely narrow curve with a width that depends on the spot size of the incident beam and the detector area. An ideal specular curve with no haze resembles a dirac-delta function. Surfaces like transparent paper or Ag NW networks possess a dense fibrous network that have large scattering cross-sections emanating from each nanostructure, where the diffuse component dominates resulting in broadened angular distribution.

The scattering angle distributions were measured with a detector rotating behind sample surfaces illuminated with a 532 nm semiconductor laser. Measurements for an ITO sample sputtered on soda-lime glass (Fig. 4(a)), a transparent paper substrate (Fig. 4(b)), and the Ag NW transparent conducting paper sample evaluated in the previous section (Fig. 4(c)) were

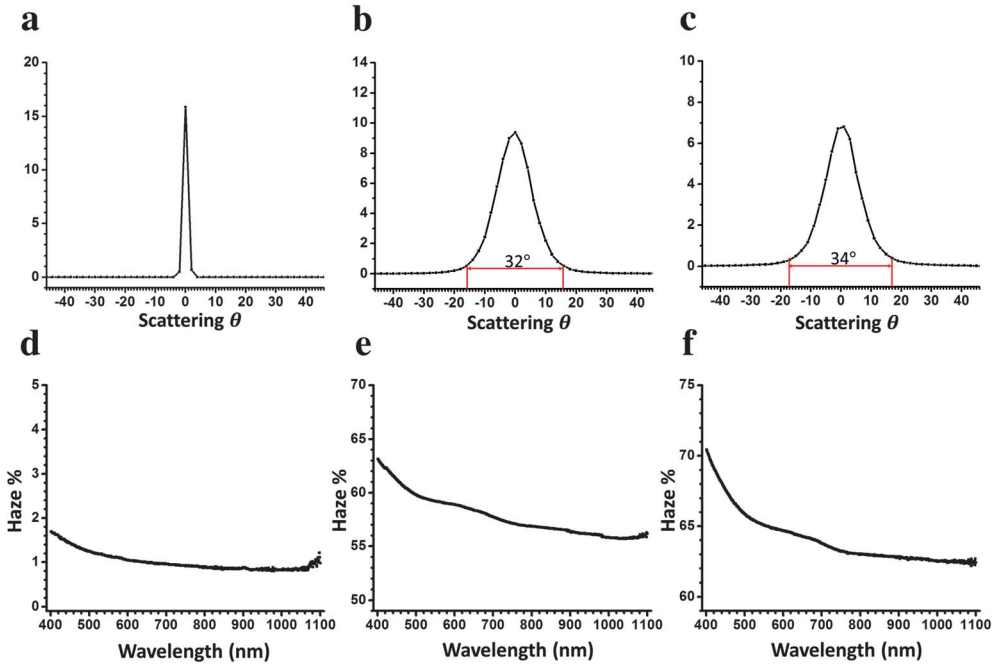

Fig. 4 Diffuse scattering angular distribution with arbitrary *y*-axis units for (a) ITO on glass, (b) transparent paper, and (c) Ag NW paper; the total diffuse optical haze for (d) ITO on glass, (e) transparent paper, and (f) Ag NW paper.

taken with this optical setup to show the angular distribution of diffusely scattered light through each sample. As expected, for ITO the angular distribution of the transmitted light is concentrated in the incident direction, demonstrating almost entirely specular transmittance. A slight deviation from an ideal dirac-delta regression in Fig. 4(a) is due to the detector area and spot size of the incident beam, making perfect point measurements impossible for this setup. The transmission through the transparent paper substrate in Fig. 4(b) produces high diffuse scattering in a Gaussian-like pattern. The scattering angle range is defined in this paper as the scattered angles that demonstrate a light intensity greater than 5% of the peak intensity at 0°. The scattering distribution extends radially up to 16° from the axis of symmetry for the transparent paper substrate, which delivers a maximum scattering solid angle of 32°. Once the Ag NW network is embedded into the paper substrate to form the Ag NW transparent conducting paper electrode the scattering distribution extends to 17° in the radial direction from the axis of symmetry, which delivers a maximum scattering angle range of 34° as seen in Fig. 4(c).

In order to verify the total diffuse scattering of Fig. 4(f) with Fig. 4(c) the integral of the total angular distribution of the light intensity minus solid angle of the incident opening in the integrating sphere of the UV-Vis Spectrometer was taken in polar coordinates with respect to θ and rotated around the incident axis for all φ angles. It is obvious from these measurements that ITO exhibits specular transmission and no diffuse scattering phenomena were measured, while the Ag NW transparent conducting paper electrode exhibits high diffuse scattering across a wide angular range. It is also clear from these measurements that diffuse scattering properties are not restricted to the paper substrate, or just the Ag NW embedded network, but that there is a nominal contribution from each component of the hybrid structure to the optical haze as well as the maximum scattering angle range of the TCE. The additional contribution from the Ag NW network may be routed to the induced oscillations of conductive electrons at the surface plasmon resonance, which scatter light constructively with directly transmitted light in the visible and infrared region.[46,47] This enhanced scattering from the plasmonic effect of Ag NWs manifests as greater diffuse optical haze in the Ag NW paper TCE than for the paper substrate alone. Another explanation is that the Ag NW network is porous with smaller cavities of air than in transparent paper, which will increase the ratio of diffusely scattered light *versus* directly transmitted light since there is a higher probability for light scattering phenomena. The enhancement of the angular distribution by the addition of the Ag NW can be attributed to the compounding scattering mechanisms of the paper substrate and the Ag NW network.

Device applications

Photovoltaic light absorption theory. The optical haze of a TCE will contribute light trapping that can greatly increase absorption and/or reduce required material in photovoltaic devices. Despite this, haze is generally not considered when evaluating and comparing TCE's. In order to compare the above films and other standard films in terms of potential photovoltaic performance, a ray-optics simulation was created.[44] The simulation was performed with several generalizing assumptions. While these assumptions don't describe a real device, they do capture all of the important physics and give a non-arbitrary comparison of different TCE's without requiring a large number of inputs. Here we assume: (1) light is incident on

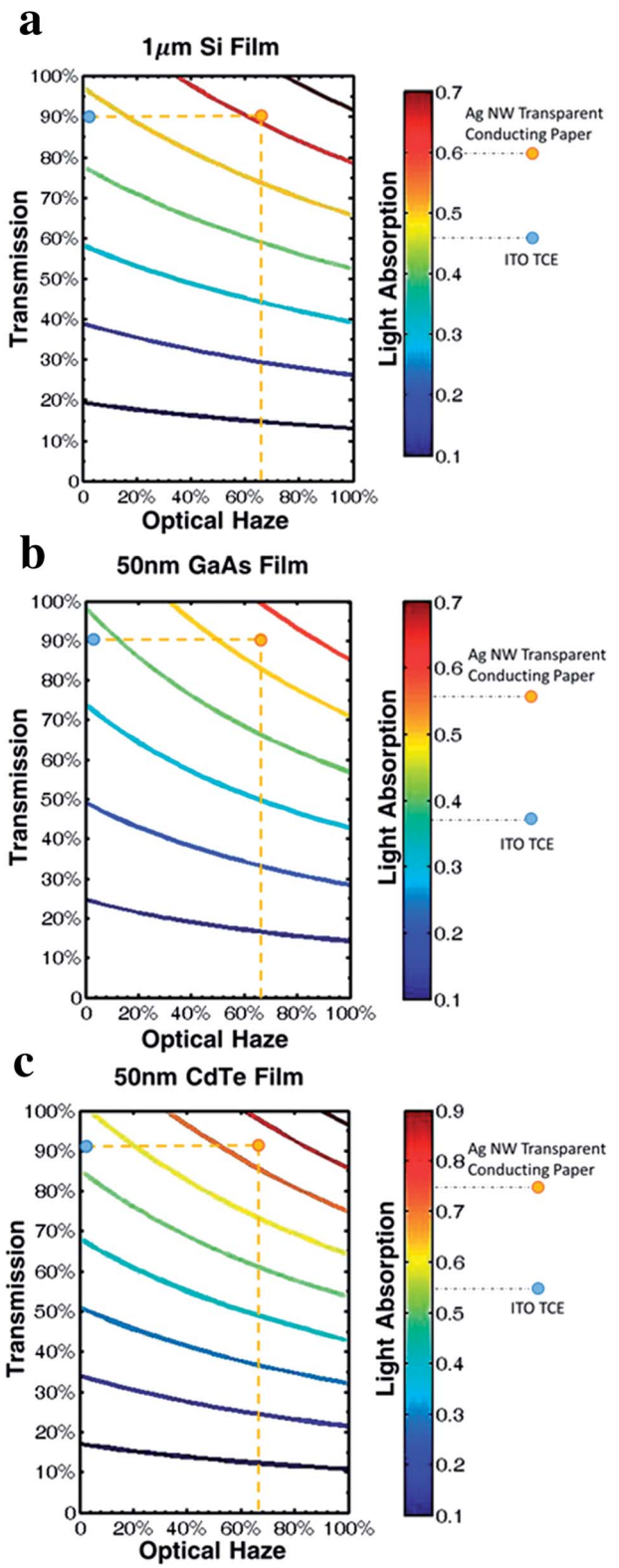

Fig. 5 Light absorption dependence of a structure including either a TCE with varying optical properties and an absorber layer (a) a 1 μm thick Si film, (b) a 50 nm thick GaAs film, and a 50 nm thick CdTe film. Light absorption in these absorbers for a highly transparent ITO TCE and our Ag NW paper TCE are compared as well.

the TCE as part of a TCE/absorber/mirror stack; (2) a fraction of light, T, is transmitted through the TCE on the first pass; (3) the angular distribution of light is then split into a diffuse component with fractional power H with cosine (Lambertian) angular dependence and a specular component with fractional power $(1 - H)$; (4) the reflection at the absorber/TCE interface is then determined by Fresnel coefficients; (5) the diffuse component undergoes Lambertian scattering at the absorber/TCE and the specular component experiences no scattering but loses coherence at the interface. The calculated absorption values are then weighted by the solar spectrum and averaged.

Photovoltaic light absorption simulation. Fig. 5 shows contour plots for the fraction of light absorbed in the absorbing layer of several simulated thin film photovoltaic structures with varied optical haze and initial transmission for the TCE.[39–42] As shown, in the region of high transmission large gains in absorption can be attained by increasing the optical haze. In addition, Fig. 5 compares a high performance ITO TCE having no optical haze but 90% transmittance, and the Ag NW transparent conducting paper with our demonstrated 65% optical haze at roughly the same transmittance as ITO. Silicon thin films demonstrate over 25% greater light absorption for structures using Ag NW transparent conducting paper rather than ITO, as illustrated in Fig. 5(a). Similarly gallium arsenide (GaAs) thin films demonstrate over 45% greater light absorption for structures using Ag NW transparent conducting paper rather than ITO [Fig. 5(b)] and cadmium telluride (CdTe) thin films demonstrate over 35% greater light absorption for structures using Ag NW paper TCE rather than ITO [Fig. 5(c)]. It is clear that Ag NW transparent conducting paper induce significantly more light absorption in thin film photovoltaic absorbers than ITO TCEs.

Conclusion

A new highly stable TCE structure composed of an Ag NW network embedded into the surface of transparent paper was achieved and its optoelectronic properties were investigated. Compared to ITO TCEs, the materials and manufacturing methods of the TCE reported in this study is cheaper, more flexible, and more amenable to large scale manufacturing. It was demonstrated that the Ag NW transparent conducting electrode exhibits better optoelectronic properties according to conventional TCE performance models, and is projected to induce greater light absorption in thin film photovoltaic absorbers than ITO TCEs due to its greater optical haze. There is conclusive evidence from the data in this investigation that Ag NW transparent conducting electrodes are an optimal replacement for ITO TCEs in thin film photovoltaics based on their superior individual performance and projected enhancement of solar device performance.

Experimental methods

Synthesis of Ag NW transparent conducting paper electrode

A reported method by Fang *et al.* was used to form transparent paper from TEMPO-treated wood pulp (1 wt%) with a highly smooth NFC surface.[43,45] A 10 mg ml^{-1} Ag NW suspension was

diluted into 0.1 mg ml^{-1} with ethanol and filtered onto the transparent paper to form a uniform Ag NW film. Finally, the Ag NW film was laminated with the pure NFC layer of the above-mentioned transparent paper, and the laminated paper was placed between regular filter papers to absorb residue water within the wet sheet and dried at room temperature under pressure.

Instruments and characterization

The SEM images were taken with a Hitachi SU-70 Analytical UHR FEG-SEM. The total transmittance and total diffuse optical haze was measured with a PerkinElmer Lambda 35 UV-Vis Spectrometer with a Labsphere RSA-ES-20 integrating sphere. The sheet resistance was measured with a four-point probe.

Acknowledgements

L. Hu would like to acknowledge the AFOSR Young Investigator program. J. N. Munday would like to acknowledge the Minta Martin award. Zhiqiang Fang would like to thank the China Scholarship Council (CSC) for their financial support. The authors would also like to acknowledge the Maryland Nanocenter and its NISP lab, which is supported by the NSF as a MRSEC Shared Experimental Facility.

References

1 M. Rowell and M. McGehee, *Energy Environ. Sci.*, 2011, **4**(1), 131.
2 G. Koishiyev and J. Sites, *Sol. Energy Mater. Sol. Cells*, 2009, **93**(3), 350–354.
3 U. Bach, D. Lupo, P. Comte, J. Moser, F. Weissortel, J. Salbeck, H. Spreitzer and M. Gratzel, *Nature*, 1998, **395**, 583.
4 S. De, T. Higgins, P. Lyons, E. Doherty, P. Nimalraj, W. Blau, J. Boland and J. Coleman, *ACS Nano*, 2009, **3**, 1767.
5 Z. Chen, B. Cotterell, W. Wang, E. Guenther and S. Chua, A mechanical assessment of flexible optoelectronic devices, *Thin Solid Films*, 2011, 202–206.
6 A. Kumar and C. Zhou, *ACS Nano*, 2010, **4**, 11.
7 G. Gruner, *J. Mater. Chem.*, 2006, **16**, 3533.
8 Z. Wu, Z. Chen, Z. Du, J. Logan, J. Sippel, M. Nikolou, K. Kamaras, J. Reynolds, D. Tanner, A. Hebard and A. Rinzler, *Science*, 2004, **305**, 1273.
9 M. Zhang, S. Fang, A. Zakhidov, S. Lee, A. Aliev, C. Williams, K. Atkinson and R. Baughman, *Science*, 2005, **309**, 1215–1219.
10 L. Hu, D. Hecht and G. Gruner, *Nano Lett.*, 2004, **4**, 2513.
11 K. Kim, Y. Zhao, H. Jang, S. Lee, J. Kim, K. Kim, J. Ahn, P. Kim, J. Choi and B. Hong, *Nature*, 2009, **457**, 706.
12 A. Geim and K. Novoselov, The rise of graphene, *Nat. Mater.*, 2007, **6**, 183.
13 G. Eda, G. Fanchini and M. Chhowalla, *Nat. Nanotechnol.*, 2008, **3**, 270.
14 C. Liu and X. Yu, *Nanoscale Res. Lett.*, 2011, **6**, 75–87.
15 A. Madaria, A. Kumar, F. Ishikawa and C. Zhou, *Nano Res.*, 2010, **3**, 564.
16 J. Groep, P. Spinelli and A. Polman, *Nano Lett.*, 2012, **12**, 3138.
17 H. Wu, L. Hu, M. Rowell, D. Kong, J. Cha, J. McDonough, J. Zhu, Y. Yang, M. McGehee and Y. Cui, *Nano Lett.*, 2010, **10**, 4242.
18 L. Hu, H. Kim, J. Lee, P. Peumans and Y. Cui, *ACS Nano*, 2010, **4**, 2955.
19 Y. Sun, *Nanoscale*, 2010, **2**, 1626.
20 J. Lee, Connor, Y. Cui and P. Peumans, *Nano Lett.*, 2008, **8**, 689.
21 D. Tobjörk and R. Österbacka, *Adv. Mater.*, 2011, **23**, 1935–1961.
22 M. Nogi, S. Iwamoto, A. N. Nakagaito and H. Yano, *Adv. Mater.*, 2009, **21**, 1595–1598.
23 Y. Okahisa, A. Yoshida, S. Miyaguchi and H. Yano, *Compos. Sci. Technol.*, 2009, **69**, 1958–1961.
24 H. Zhu, S. Parvinian, C. Preston, O. Vaaland, Z. Ruan and L. Hu, *Nanoscale*, 2013, **5**, 3787–3792.
25 J. Huang, H. Zhu, Y. Chen, C. Preston, K. Rohrbach, J. Cumings and L. Hu, *ACS Nano*, 2013, **7**(3), 2106–2113.
26 C. Preston, Y. Xu, X. Han, J. Munday and L. Hu, *Nano Res.*, 2013, **6**(7), 461–468.
27 F. Xu and Y. Zhu, *Adv. Mater.*, 2012, **24**, 5117–5122.
28 D. Hecht, L. Hu and G. Irvin, *Adv. Mater.*, 2011, **23**(13), 1482–1513.
29 S. Sepulveda-Mora and S. Cloutier, *J. Nanomater.*, 2012, 1–7.
30 Y. Feng, X. Ju, W. Feng, H. Zhang, Y. Cheng, J. Liu and A. Fujii, *Appl. Phys. Lett.*, 2012, **94**(12), 123302.
31 X. Li, Y. Zhu, W. Cai, M. Borysiak, B. Han, D. Chen and R. Piner, *Nano Lett.*, 2009, **9**(12), 4359–4363.
32 M. Kang, M. Kim, J. Kim and L. Guo, *Adv. Mater.*, 2008, **20**(23), 4408–4413.
33 Y. Galagan, J. Rubingh, R. Andriessen, C. Fan, P. Blom, S. C. Veenstra and J. Kroon, *Sol. Energy Mater. Sol. Cells*, 2011, **95**(5), 1339–1343.
34 S. Wang, X. Zhang and W. Zhao, *J. Nanomater.*, 2013, 1–6.
35 Q. Zheng, B. Zhang, X. Lin, X. Shen, N. Yousefi, Z. Huang and Z. Li, *J. Mater. Chem.*, 2012, **22**(48), 25072.
36 F. Xu and Y. Zhu, *Adv. Mater.*, 2012, **24**(37), 5117–5122.
37 W. Hu, X. Niu, L. Li, S. Yun, Z. Yu and Q. Pei, *Nanotechnology*, 2012, **23**(34), 344002.
38 M. Nieto-Vesperinas, *Scattering and Diffraction in Physical Optics*, World Scientific Publishing Co, 2006.
39 K. Yamamoto, M. Yoshimi, Y. Tawada, Y. Okamoto, A. Nakajima and S. Igari, *Appl. Phys. A: Mater. Sci. Process.*, 1999, **69**(2), 179–185.
40 J. Yoon, S. Jo, I. Chun, I. Jung, H. Kim, M. Meitl, E. Menard, X. Li, J. Coleman, U. Paik and J. Rogers, *Nature*, 2010, **465**, 329–330.
41 K. Chopra, P. Paulson and V. Dutta, *Prog. Photovoltaics*, 2004, **12**, 69–92.
42 N. Paudel, K. Wieland and A. Compaan, *Sol. Energy Mater. Sol. Cells*, 2012, **105**, 109–112.
43 Z. Fang, H. Zhu, C. Preston, X. Han, Y. Li, S. Lee, X. Chai, G. Chen and L. Hu, *J. Mater. Chem. C*, 2013, **1**, 6191–6197.
44 J. Murray, C. Preston, L. Hu and J. N. Munday, Effects of Transparent Conducting Electrode Haze on Thin Film Solar Cell Efficiency, in preparation.

45 Z. Fang, H. Zhu, D. Ha, C. Preston, Q. Chen, S. Lacey, Y. Li, X. Han, S. Lee, G. Chen, X. Chai, J. N. Munday and L. Hu, Paper with Ultra-High Transparency and Ultra-High Haze for Solar Cells, submitted.
46 J. Groep, P. Spinelli and A. Polman, *Nano Lett.*, 2012, **12**, 3138–3144.
47 K. Catchpole and A. Polman, *Opt. Express*, 2008, **16**(26), 2173–2180.